

1 **Forest responses to last-millennium hydroclimate variability are governed by spatial**
2 **variations in ecosystem sensitivity**
3

4 **Authors:**

- 5 1. **Christine R. Rollinson***, crollinson@mortonarb.org
6 a. Center for Tree Science, The Morton Arboretum, 4100 Illinois Route 53, Lisle, IL,
7 60532
8 2. **Andria Dawson**, andria.dawson@gmail.com
9 a. Department of General Education, Mount Royal University, Calgary, Alberta, T3E
10 6K6, Canada
11 3. **Ann M. Raiho**, ann.raiho@gmail.com
12 a. Department of Biological Sciences, University of Notre Dame, 100 Galvin Life
13 Science Center, Notre Dame, IN, 46556,
14 4. **John W. Williams**, jwilliams1@wisc.edu, jww@geography.wisc.edu
15 a. Department of Geography and Center for Climatic Research, University of
16 Wisconsin-Madison, Madison, WI 53704
17 5. **Michael C. Dietze**, dietze@bu.edu orcid:0000-0002-2324-2518
18 a. Department of Earth and Environment, Boston University, 685 Commonwealth
19 Ave, Boston, MA 02215
20 6. **Thomas Hickler**, thomas.hickler@senckenberg.de
21 a. Senckenberg Biodiversity and Climate Research Centre (SBIK-F),
22 Senckenberganlage 25, 60325 Frankfurt/Main, Germany
23 b. Department of Physical Geography, Goethe University, Frankfurt/Main, Germany
24 7. **Stephen T. Jackson**, jackson@uwyo.edu; stjackson@usgs.gov
25 a. Southwest Climate Adaptation Science Center, US Geological Survey,
26 b. Department of Geosciences, University of Arizona, Tucson, AZ 85721
27 8. **Jason McLachlan**, Jason.S.McLachlan.2@nd.edu, jmclachl@nd.edu
28 a. Department of Biological Sciences, University of Notre Dame, 100 Galvin Life
29 Science Center, Notre Dame, IN, 46556
30 9. **David JP Moore**, davidjpmoore@email.arizona.edu
31 a. School of Natural Resources, University of Arizona, Tucson, AZ, 85721
32 10. **Benjamin Poulter**, benjamin.poulter@nasa.gov
33 a. NASA GSFC, Biospheric Sciences Lab., Greenbelt, MD 20771
34 11. **Tristan Quaife**, t.i.quaife@reading.ac.uk
35 a. Department of Meteorology, University of Reading, Reading, RG6 6BB UK
36 12. **Jörg Steinkamp**, steinkamp.joerg@gmail.com
37 a. Senckenberg Biodiversity and Climate Research Centre (SBIK-F),
38 Frankfurt/Main, Germany
39 b. Johannes Gutenberg University, Mainz, Germany
40 13. **Mathias Trachsel**, mtrachs@gmail.com
41 a. Department of Geography, University of Wisconsin-Madison, Madison, WI 53704
42

43 **Running Title**
44 Past forest variability and sensitivity

45
46 **Keywords**
47 stability, vulnerability, drought, ecosystem modeling, paleoecology, climate change,
48

49 **Statement of Authorship:**
50 CRR, AD, AMR, and JWW designed the study. AD, AMR, JWW, STJ, JM, and MT created
51 pollen reconstructions and aided in interpretation (STEPPS, ReFAB). AD and AMR wrote the
52 pollen methods. CRR, AMR, MCD, JM, DJPM, BP, TQ, and JS performed ecosystem model
53 simulations and aided in interpretation. CRR and JWW wrote the manuscript with additional
54 input from AD, AMR, and all authors.
55

56 **Data Accessibility Statement:**
57 Should the manuscript be accepted, the data supporting the results will be archived in two
58 public repositories and the DOIs will be included at the end of this article. Pollen data is already
59 available or will be made available upon acceptance on the EDI data portal as an msb-paleon
60 product. The [Environmental Data Initiative](#) is an NSF-funded program tailored towards
61 environmental data and works closely with the US Long-Term Ecological Research (LTER)
62 Network, NSF Macrosystems Biology program (which funded our work), and DataONE.
63 Terrestrial ecosystem model drivers and output are in the process of being archived on the
64 ORNL DAAC. The [Oak Ridge National Laboratory Distributed Active Archive Center \(ORNL
65 DAAC\)](#) is managed by NASA's Earth Science Data and Information Systems program and is
66 best-suited to archiving ecosystem model output, which is often large and has converged on
67 netcdf as a standard file format. These repositories have been approved by *Ecology Letters*
68 editorial staff. All code for analyses is publicly available on Github: [https://github.com/PalEON-
69 Project/EcosystemVariability](https://github.com/PalEON-Project/EcosystemVariability)
70

71 **Manuscript Metadata:**
72 **Abstract Word Count:** 150
73 **Manuscript Word Count:** 4,542
74 **Text Box Word Count:** N/A
75 **Number of References:** 62
76 **Number of Figures:** 4
77 **Number of Tables:** 1
78 **Number of Text Boxes:** 0
79

80 **Corresponding Author:** Christine R. Rollinson, Center for Tree Science, The Morton
81 Arboretum, 4100 Illinois Route 53, Lisle, IL 60532; phone: 630-719-2422; email:
82 crollinson@mortonarb.org
83

84 **Abstract**

85 Forecasts of forest responses to climate variability are governed by climate exposure and
86 ecosystem sensitivity, but ecosystem model projections and process representations are under-
87 constrained by data at multidecadal and longer timescales. Here, we assess ecosystem
88 sensitivity to centennial-scale hydroclimate variability, by comparing dendroclimatic and pollen-
89 inferred reconstructions of drought, forest composition and biomass for the last millennium with
90 five ecosystem model simulations. In both observations and models, spatial patterns in
91 ecosystem responses to hydroclimate variability are strongly governed by ecosystem sensitivity
92 rather than climate exposure. Ecosystem sensitivity was highest in simpler models and higher
93 than observations, suggesting that interactions among biodiversity, demography, and
94 ecophysiology processes dampen the sensitivity of forest composition and biomass to climate
95 variability and change. By integrating ecosystem models with observations from timescales
96 extending beyond the instrumental record, we can better understand and forecast the
97 mechanisms regulating forest sensitivity to climate variability in a complex and changing world.
98

99 **Introduction**

100 Exposure to 21st-century climate change is expected to profoundly impact global forest
101 composition, diversity, and structure (Dawson *et al.* 2011; Keeley *et al.* 2019), but the sensitivity
102 of ecosystems to climate variability at multi-decadal to centennial time scales is poorly
103 constrained by instrumental observations. Multiple observational studies that employ
104 subcontinental- to continental-scale data networks across a broad range of timescales have
105 sought to empirically estimate the sensitivity of forest ecosystems to climate variability. The
106 sensitivity of tree growth rates, biomass accumulation, and ecophysiological processes to
107 interannual climate variability is well-documented by dendroecological data, with compelling
108 evidence that forest sensitivity to climate depends on forest age and is non-stationary across
109 space and time (Charney *et al.* 2016; Klesse *et al.* 2018; Thom *et al.* 2019; Peltier & Ogle
110 2020). On glacial-interglacial timescales, networks of fossil pollen records show that
111 temperature variations are the primary driver of forest composition and species distributions
112 (Shuman *et al.* 2004; Nolan *et al.* 2018), while over the last several thousand years,
113 hydroclimate variability has strongly affected forest composition and structure in temperate
114 forests of the northeastern and upper midwestern United States (Booth *et al.* 2012; Shuman *et*
115 *al.* 2019).

116 Terrestrial ecosystem models used to forecast responses to climate change often have
117 difficulty reproducing broad-scale and long-term responses to environmental variability, despite
118 being well-grounded in empirical evidence and ecological theory (Friedlingstein *et al.* 2006,
119 2014; Matthes *et al.* 2016). These models mechanistically connect ecophysiological processes
120 and climate variability to past and present changes in forest composition and structure, but are
121 subject to uncertainty in external forcings (e.g. drivers), process representation, and
122 parametrization that complicates data-model comparisons (Figure 1) (LeBauer *et al.* 2013;
123 Matthes *et al.* 2016; Dietze 2017; McLachlan & PalEON Project 2018). Each model includes
124 hypotheses about the primary processes and ecosystem characteristics governing forest

125 change, various simplifying assumptions, and tradeoffs between computational tractability and
126 process complexity (De Kauwe *et al.* 2013; Walker *et al.* 2014; Medlyn *et al.* 2015). Previous
127 data-model comparisons have returned mixed evidence about whether models underestimate or
128 overestimate the sensitivity of forest processes such as net primary productivity (NPP) and
129 mortality to climate change (Schimel *et al.* 2015; Walker *et al.* 2015; Rollinson *et al.* 2017). As a
130 result, projections of forest compositional and structural responses to climate change have high
131 uncertainty, limiting their utility for ecological forecasting and science-based adaptation
132 (Friedlingstein *et al.* 2014).

133 Several challenges have traditionally hindered the joint analysis and integration of
134 terrestrial ecosystem models and paleoecological data to better constrain modeled responses to
135 climate variations at multi-decadal and longer timescales. First, the raw observations collected
136 from fossil pollen records (counts of individual pollen taxa) have no direct counterparts in
137 ecosystem models. Bayesian hierarchical models are providing new process-based
138 approaches to infer emergent ecosystem properties from fossil pollen records, such as forest
139 composition, diversity, percent cover, and biomass (Raiho *et al.* in prep; Blarquez & Aleman
140 2016; Dawson *et al.* 2016), but the number of state variables that can be estimated from
141 paleoecological data remains small relative to the number of latent (i.e. unobservable) variables
142 simulated by ecosystem models (Fig. 1). Second, pre-instrumental model-data comparisons
143 are complicated by reliance on driver datasets derived from general circulation models (GCMs).
144 GCMs generally capture macroscale spatial patterns and low-frequency trends in climate but
145 are unable to fully capture the complexity and stochasticity of local to regional-scale weather
146 phenomena at the subdaily resolution needed to drive ecosystem models, resulting in
147 systematic spatial and temporal biases in model simulations (Anav *et al.* 2013; Matthes *et al.*
148 2016; Dietze *et al.* 2018). Third, the native temporal resolution varies between paleodata and
149 models and requires a temporal standardization. Due to these challenges, the predicted
150 sensitivity of ecosystem model state variables such as forest composition and biomass to

151 climate change is largely unvalidated by observations at multidecadal and longer timescales,
152 resulting in wide divergence among terrestrial ecosystem models in their 21st-century
153 projections (Friedlingstein *et al.* 2006, 2014). Fourth, terrestrial ecosystem models vary widely in
154 represented processes, which can challenge intermodel comparisons but also provide insight
155 into key governing ecological processes when data-model discrepancies emerge.

156 Here, we seek to establish the patterns of forest ecosystem and climate variability in the
157 north-central and northeastern US for the last millennium (850-1850 C.E.) and identify the
158 mechanisms underpinning both forest ecosystem sensitivity and observed data-model
159 discrepancies. In these analyses, we test hypotheses about the relative importance of
160 hydroclimate exposure and climate sensitivity as determinants of ecosystem variability. We also
161 hypothesize that ecosystem models will be overly sensitive to hydroclimate variability due to
162 insufficient representation of ecophysiological and demographic processes that can dampen
163 climate responses. To this end, we present a novel series of data-model and model-model
164 comparisons that are designed to overcome traditional barriers to data-model intercomparison
165 for pre-instrumental times. Our analyses combine dendroclimatic indices of drought, recently
166 published Bayesian spatiotemporal estimates of forest composition and biomass derived from
167 pollen that provide independent checks on last-millennium simulations from five terrestrial
168 ecosystem models for the northeastern and upper midwestern United States. The data-model
169 comparisons discriminate among differing representations of forest processes, while the model-
170 model comparisons help diagnose causal relationships among ecological processes, changes in
171 forest states, and climate variability (Fig. 1). To test hypotheses while also overcoming known
172 geographic biases in the model simulations of ecosystem state such as forest composition that
173 source back to biases in the climate model drivers (Matthes *et al.* 2016), we develop a new
174 variability metric that we apply to the data and model-derived products that focuses on
175 comparisons among variability of hydroclimate, composition, and biomass (Fig. 1). Our results
176 indicate that at centennial timescales, spatial patterns in the variability of forest composition and

177 biomass are regulated by ecological factors such as ecotonal position and complexity rather
178 than climate exposure as defined by the local magnitude of climate variability.

179

180 **Materials & Methods**

181 *Overview*

182 We employ a combination of data-model and model-model comparisons (Fig. 1) in which
183 we combine paleoclimatic and paleoecological datasets to draw inferences about past variations
184 in hydroclimate and forest composition and biomass. The temporal domain of this study is 850-
185 1850 AD and is bounded by the temporal extent of the climate drivers (850 AD) and time of
186 settlement-era tree surveys (ca. 1850 AD). In our study, 'data' refers to observation-based
187 statistical models of past drought, forest composition, and biomass, reconstructed from tree
188 rings, historical tree surveys, and networks of fossil pollen records. These data-based
189 inferences are fully independent of the ecosystem model simulations. Model-based
190 comparisons are from the PalEON Ecosystem Model Intercomparison Project (PEMIP)
191 (Rollinson *et al.* 2017), which used spatially and temporally downscaled past climate simulations
192 from the Fifth Coupled Model Intercomparison Project (CMIP5) as drivers. Comparisons among
193 ecosystem model simulations and empirical data rely on normalized values compared in
194 environmental space, rather than geographic space, in order to reduce the effects of any bias in
195 the climate drivers in our analyses and to focus on sensitivity of ecosystems to climate variability
196 (Supplemental Figure 1).

197

198 *Observational Datasets*

199 The inferred datasets leverage recent advances in pollen-vegetation modeling (Dawson
200 *et al.* 2016), a form of proxy system modeling (Evans *et al.* 2013) in which ecosystem state
201 variables such as composition and biomass are estimated along with associated observational
202 uncertainties. Of the three inferred datasets used here, two were derived from networks of

203 fossil pollen records provided by individual data contributors and the Neotoma Paleocology
204 Database and were calibrated against historical surveys of forest composition and structure
205 from the early stages of EuroAmerican settlement (Liu *et al.* 2011; Dawson *et al.* 2016; Goring
206 *et al.* 2016; Kujawa *et al.* 2016; Paciorek *et al.* 2016). Pollen-based inferences are based on
207 statistical pollen-vegetation models (PVMs) called STEPPS and ReFAB, and represent
208 fractional vegetation composition and total woody biomass, respectively, for 12 tree genera that
209 are common elements of upper Midwest forests. STEPPS is a Bayesian hierarchical spatio-
210 temporal model that infers fractional forest composition from networks of fossil pollen records
211 (Paciorek & McLachlan 2009; Dawson *et al.* 2016, 2019b; Trachsel *et al.* 2020). STEPPS
212 employs a process-based representation of pollen dispersal and production, with taxon-specific
213 parameterizations. STEPPS is calibrated using spatial datasets of pollen samples and forest
214 composition data, here from the settlement era ((Paciorek & McLachlan 2009; Dawson *et al.*
215 2016), then run for fossil pollen assemblages for other time intervals to produce posterior
216 estimates of past forest composition. Using this framework, STEPPS: (i) explicitly characterizes
217 uncertainty in data and processes, with posterior distributions of process parameters and state
218 variables such as forest composition, and (ii) borrows information across space and time,
219 allowing for spatially comprehensive estimates of composition. For both the upper Midwestern
220 USA (UMW; Minnesota, Wisconsin, Michigan) (Dawson *et al.* 2019a) and the northeastern USA
221 (NEUS) (Trachsel *et al.* 2020), STEPPS has been used to estimate centennially-resolved forest
222 composition for the late Holocene (250 B.C. to 1750 A.D) at a 24 km grid; here we use the
223 results from 850 to 1750 AD.

224 ReFAB also employs a similar approach to STEPPS, but focuses specifically on
225 estimating total aboveground woody biomass (Raiho *et al.* in prep). ReFAB is calibrated using
226 the relationship between settlement-era multivariate pollen counts and biomass from PLS
227 surveys (Paciorek *et al.* 2019). Parameter estimates from calibration are then used to
228 reconstruct centennially resolved biomass for 77 sites in the UMW for the last 10,000 years

229 (Raiho *et al.* in prep). ReFAB can characterize the uncertainty in sediment pollen age estimates,
230 calibration parameters, the relationship between species composition and total aboveground
231 woody biomass, and species-level allometries.

232 The Living Blended Drought Atlas (LBDA) provides yearly estimates of summer (mean
233 June, July, August) Palmer Severity Drought Index (PDSI) for North America, based on
234 networks of tree-growth chronologies (Cook *et al.* 2010; Woodhouse *et al.* 2010). We used
235 PDSI as our measure of climate variability, because PDSI is an important predictor of forest
236 dynamics in this domain and can also be calculated directly from the meteorological forcings
237 used for the ecosystem model simulations (Clifford & Booth 2015; Cook *et al.* 2015). LBDA
238 PDSIs are provided at 0.5-degree spatial grid resolution. Due to varying temporal extent of tree-
239 growth chronologies, the temporal extent of the LBDA varies. The earliest years in this spatial
240 domain ranged from 0 to 1671 AD, while the latest year was 2005 (Supplemental Figure 1).

241

242 *Modeling Datasets*

243 PEMIP model simulations here comprised five ecosystem models (ED2; LINKAGES;
244 LPG-WSL; LPJ-GUESS; and JULES-TRIFFID) with dynamic vegetation run at 254 locations
245 across the eastern and midwestern US at 0.5-degree spatial resolution. These models vary in
246 how they characterize forest composition and carbon dynamics and range from species-based
247 with little ecophysiological process representation (e.g. LINKAGES) to detailed ecophysiology
248 and cohort representation, but reliance on plant functional types (PFTs; e.g. ED2, Table 1). LPJ-
249 GUESS and LPJ-WSL both included stochastic fire disturbances in their simulations, while other
250 models such as ED and LINKAGES include processes of tree mortality that assume landscape-
251 scale equilibrium (Rollinson *et al.* 2017).

252 The PEMIP climate drivers were developed following a standard protocol (Rollinson *et*
253 *al.* 2017, Supplemental Figure 1). CCSM4 output from the Paleoclimate Modeling
254 Intercomparison Project, Phase III (PMIP3) past millennium simulations and the Coupled Model

255 Intercomparison Project, Phase 5 (CMIP5) historical simulations were downscaled to 0.5-degree
256 spatial resolution and 6-hourly temporal resolution using standard protocols (Kumar *et al.* 2012;
257 Rollinson *et al.* 2017). Soil texture is from the Harmonized World Soil Database (Wei *et al.*
258 2014). After the 6-hourly PEMIP climate driver datasets were created, they were then
259 temporally averaged to meet the specific driver requirements of individual ecosystem models,
260 which vary in temporal resolution. ED2 and JULES-TRIFFID use the full suite of 6-hourly
261 drivers for temperature, precipitation, shortwave radiation, longwave radiation, surface pressure,
262 specific humidity, wind speed, and carbon dioxide concentration. Meteorological drivers for the
263 two LPJ variants include daily temperature, precipitation, and shortwave radiation plus longwave
264 radiation for LPJ-WSL. LINKAGES only requires monthly average temperature and
265 precipitation. Monthly temperature and precipitation were combined with soil water holding
266 capacity computed from model driver soil texture and depth to calculate PDSI, following (Cook
267 *et al.* 2015), but using the Thornthwaite equation for evapotranspiration (Thornthwaite & Mather
268 1957; Pelton *et al.* 1960) due to evapotranspiration varying among ecosystem models given the
269 same temperature and precipitation drivers as a results of differences in model structure and
270 parameterization. From the ecosystem models we extracted two variables that can be
271 compared to paleoecological observations (fractional forest composition and biomass) and four
272 latent variables (Fig. 1): gross primary productivity (GPP), net primary productivity (NPP), net
273 ecosystem exchange (NEE), and leaf area index (LAI).

274

275 *Analyses*

276 Analyses focused on the comparison of empirical data and ecosystem model outputs of
277 centennial-scale variability in forest composition and biomass driven by drought variability over
278 the last 1,000 years. We first ensured temporal comparability by transforming or aggregating
279 variables to a common centennial resolution. Second, we developed common metrics of

280 ecosystem and drought variability to support data-model and model-model intercomparisons
281 and to minimize the potential effects of climate model driver bias.

282 With respect to temporal compatibility, STEPPS and ReFAB datasets are natively at
283 100-year resolution and variability was calculated as the mean of the absolute first differences
284 between adjacent time points, using all posterior draws from these datasets and then calculating
285 the mean variability value across posterior draws. For the annually resolved datasets (all model
286 output, drivers, and LBDA), a generalized additive model (GAM) was used to smooth these time
287 series to a centennial-scale resolution. For the GAM, we predicted the response variable (e.g.
288 drought, biomass, GPP) as a function of time (year) as a thin-plate regression spline with one
289 knot per 100 years using the *gam* function in the *mgcv* package in R (Wood 2017; Simpson
290 2018). From the GAM, we generated a 1000-member posterior distribution of each predicted
291 variable through time using the error and covariance of the intercept and spline parameters. We
292 then extracted the predicted values at 100-year intervals and calculated variability as described
293 for STEPPS and ReFAB.

294 For the second step, we developed two common metrics for our comparisons: mean
295 relative variability and sensitivity to hydroclimate variability. Mean relative variability was
296 calculated by normalizing all variability values by dividing by the mean for the variable across
297 the dataset (i.e. across all spatiotemporal loci for a given combination of variable and model or
298 observational dataset). This normalization is intended to facilitate comparison among variables
299 with different units and scales. Because each grid cell had multiple taxa, for the compositional
300 response variable we used the variability of the taxon or plant functional type with the highest
301 fractional composition at each location. Sensitivity to hydroclimate variability was quantified as
302 the slope of a linear regression between variability as the independent variable and variability of
303 the ecosystem response variable such as composition or biomass. These analyses always
304 used the appropriate observational or modeled PDSI variability (i.e. LBDA for the pollen-inferred
305 compositional variability; calculated PEMIP driver PDSI variability for the model-simulated

306 compositional variability) to ensure internal consistency between climatic forcing and ecosystem
307 response. For all analyses and presented results, normalized variability is log-transformed to
308 meet standard statistical assumptions of Gaussian distributions and homoscedasticity.

309

310 **Results**

311 In the observational data, variability in forest composition or biomass in the northeastern
312 US (NEUS) and upper midwestern US (UMW), did not correlate to drought variability (Table 1,
313 Figs. 2, 3) in contrast with the hypothesis that high exposure to climate variability should lead to
314 increased compositional variability. Neither the full spatiotemporal domain (Table 1) nor the
315 UMW (Fig. 3, sensitivity slope = 0.010 SE 0.018) showed a significant relationship between
316 reconstructed drought and composition variability, although the NEUS showed weak sensitivity
317 (Fig. 3, sensitivity slope = 0.065 SE 0.027). Reconstructed biomass variability (Fig 2., biomass
318 reconstructions not available for the NEUS, (Paciorek *et al.* 2019)) also was uncorrelated to
319 drought variability (Table 1) and instead showed the highest variability at the historic prairie-
320 forest ecotone (Fig. 2) (Goring & Williams 2017). In pollen-based reconstructions, composition
321 and biomass variability were weakly but positively related (Fig. 3c, $R^2=0.09$, slope=0.479 SE
322 0.187) and locations with higher taxonomic richness tended to have higher variability
323 (Supplemental Fig. 2).

324 Modeled ecosystem sensitivity to drought variability was generally similar to or higher
325 than observations, with less-complex models tending to have a too-high predicted sensitivity
326 relative to the empirical reconstructions (Fig. 3). Composition variability was more sensitive to
327 drought variability than in reconstructions for three of five ecosystem models (ED2, LPJ-WSL,
328 and TRIFFID), with the data-model discrepancy most pronounced in models with fewer plant
329 types or taxa (Fig. 3a, Table 1). JULES-TRIFFID, which had only two tree PFTs (deciduous and
330 evergreen), had the highest drought sensitivity (composition slope = -8.633 SE = 1.075,
331 composition sensitivity slope 0.411 SE = 0.022). LPJ-WSL and ED2, with respectively six and

332 five PFTs, had similar mean compositional variability (LPJ-WSL slope = -7.829 SE = 0.943, ED2
333 slope = -7.156 SE = 0.514), although LPJ-WSL was approximately twice as sensitive to
334 hydroclimate variability as ED2 (Fig. 3a, Table 1, LPJ-WSL slope = 0.252 SE = 0.018, ED2 slope
335 = 0.118 SE = 0.018). LINKAGES, which simulated 15 individual species, had among the lowest
336 sensitivity to drought variability (Fig. 3a, Table 1, composition slope = -6.598 SE = 0.478,
337 composition sensitivity slope 0.074 SE = 0.018).

338 Ecosystem models with simpler representation of vegetation ecophysiology (LINKAGES,
339 JULES-TRIFFID) also had a too-high sensitivity of biomass to drought variability relative to
340 empirical reconstructions (Table 1, Fig. 3b). Both LINKAGES and JULES-TRIFFID showed a
341 tight positive coupling of biomass sensitivity to drought variability, which corresponded to strong
342 correlations between biomass and composition variability (Fig. 3c). LINKAGES showed a one-
343 to-one relationship between composition and biomass variability, which is much stronger than
344 reconstructions (Fig. 3c). Of all the models, only LPJ-WSL was consistent with the data in
345 showing a weakly negative relationship between biomass and PDSI variability (Fig. 3b) while
346 also showing a positive correlation between biomass and composition variability (Fig. 3c).

347 Further analysis of latent variables in the ecosystem models confirmed that variations in
348 modeled ecosystem sensitivity to hydroclimate variability is linked to model complexity of
349 ecosystem composition and processes (Fig. 4). There is a cascading series of linkages in
350 physiological variables within and among taxa (Figs. 1, 4), in which gross primary productivity
351 (GPP) is directly influenced by temperature and moisture availability, while other state variables
352 such as net primary productivity (NPP), leaf area index (LAI), and aboveground biomass (AGB)
353 are regulated by additional downstream processes that may decouple their variability from
354 climate variability (Fig. 1). Hence, in most models, GPP variability is the most sensitive to
355 drought variability (Fig. 4, Supplemental Table 1). In all models, sensitivity of forest composition
356 to drought variability seems to be most closely linked to sensitivity of NPP. NPP sensitivity
357 tended to be higher in low-diversity models such as JULES-TRIFFID (Figure 4, Supplemental

358 Table 1). Higher diversity through more tree types or taxa was associated with higher
359 compositional variability and reduced sensitivity to drought (Figure 3, Table 1, Supplemental
360 Figure 2).

361 Models with more detailed representation of plant ecophysiology and demography (e.g.
362 ED2, the two LPJ variants) also tended to have lower biomass sensitivity to hydroclimate
363 variability (Fig. 4) and agree more closely with observations (Fig. 3). Biomass sensitivity to
364 drought variability in our model ensemble was similar to NEE sensitivity in all models except
365 LPJ-GUESS (Fig. 4, Supplemental Table 1). LINKAGES and JULES-TRIFFID may be overly
366 sensitive to hydroclimate variability for entirely different reasons. LINKAGES has a fairly simple
367 representation of ecophysiological processes while being able to represent species-level
368 demographic dynamics (Table 1). In contrast, JULES-TRIFFID contains a sophisticated
369 representation of ecophysiology but for only two tree PFTs and five PFTs total (Table 1). The
370 other models tend to be more intermediate cases, with intermediate to more sophisticated
371 representations of both ecophysiology and vegetation dynamics.

372

373 **Discussion**

374 Over the last millennium (850-1850 A.D.), both paleodata networks and model
375 simulations suggest that spatial patterns in forest composition and biomass variability in
376 northeastern and upper midwestern United States are governed more by spatial variations in
377 ecosystem sensitivity and less by spatial variations in exposure to climate variability. Ecotonal
378 regions such as the prairie-forest border have higher variability in composition and structure
379 than areas of high PDSI variability (Fig. 2). The intermodel comparisons suggest that added
380 complexity allows slow-to-change variables such as composition and biomass to be insensitive
381 to climate variability at centennial scales despite sensitivity of fast-changing ecophysiological
382 processes such as gross and net primary productivity (Fig. 4). Incorporation of ecological

383 processes and characteristics such as diversity and demography all tend to reduce simulated
384 climate sensitivity and better align simulations with observations (Figs. 3, 4).

385 These analyses represent a milestone towards the goal of more comprehensive and
386 rigorous data-model comparisons for timescales and time periods extending beyond the
387 instrumental record. Common challenges for multi-centennial data-model comparisons include
388 1) a need for process-informed statistical models of inference for paleoecological data, 2)
389 generally lower temporal resolution in paleoecological data than in model simulations and with
390 more latent variables than for the instrumental period, 3) biases in paleoclimatic simulations
391 leading to biases in ecosystem model simulations, and 4) differences among models in driver
392 datasets and represented processes. The pollen-vegetation models used in our study include
393 processes for pollen productivity and dispersal that translates relative pollen abundances into
394 metrics of forest composition and biomass that can be directly compared to those produced by
395 ecosystem models (Paciorek & McLachlan 2009; Dawson *et al.* 2016). We further increased
396 the commensurability between centennially resolved pollen-based quantifications of forest
397 change and higher-frequency information from tree rings and ecosystem models by using GAMs
398 to achieve time series with similarly temporally smoothed properties (Simpson 2018). By
399 focusing on time series variability rather than directly comparing magnitude and timing of
400 change in specific geographic locations or taxonomic groupings we were able to overcome
401 document ecosystem model biases arising from driver, process, and parameter limitations
402 (Matthes *et al.* 2016; Dietze 2017). Finally, we leveraged differences in process representation
403 among models as a means of evaluating the importance of specific ecosystem processes for
404 producing emergent patterns of climate sensitivity that are consistent with paleoecological data
405 (Medlyn *et al.* 2015; McLachlan & PalEON Project 2018).

406 Given widespread evidence that forest composition and growth is sensitive to climate
407 variability (Shuman *et al.* 2004; Allen *et al.* 2010; Thom *et al.* 2019), the reporting here of
408 generally low sensitivity of forest composition and biomass to hydroclimate in reconstructions

409 may seem surprising (Fig. 2). Several possible explanations exist. First, this apparent
410 insensitivity may be due to the temporal grain of this study: the centennially resolved temporal
411 grain of our analyses limits detection of the effects of stochastic or short-lived extreme events
412 such as sub-decadal to decadal drought, which can cause massive mortality events that affect
413 centennial-scale forest composition (Breshears *et al.* 2005; Allen *et al.* 2010; Seidl *et al.* 2011).
414 At centennial scales, the effects of extreme weather may be confounded by additional
415 punctuated disturbances such as fire and pest outbreaks that are often unrepresented in
416 ecosystem models or purely stochastic and with implicit assumptions of landscape-scale
417 equilibria (Seidl *et al.* 2011; Fisher *et al.* 2018; McCabe & Dietze 2019). Second, apparent
418 climate sensitivity might increase if the temporal extent was increased to include larger climate
419 variations during the Holocene and last deglaciation. During the Holocene, hydroclimatic
420 variability around the North Atlantic appears to have been an important driver of forest
421 compositional changes and the collapses of individual tree species (Shuman *et al.* 2019). Large
422 vegetation changes associated with the abrupt temperature variations of the Younger Dryas and
423 last deglaciation are well documented (Williams *et al.* 2011), but the temporal extent of this
424 study was constrained by the temporal extent of the last-millennium PMIP3/CMIP5 simulations
425 used to drive ecosystem models (Braconnot *et al.* 2011; Taylor *et al.* 2012). As the next
426 generation of transient Holocene simulations become available, the conclusions reached here
427 about low apparent sensitivity can be revisited. Third, this paper focuses on spatial patterns of
428 climate and ecosystem variability, whereas most prior paleoecological studies have tended to
429 focus on temporal variations (Shuman *et al.* 2004; Booth *et al.* 2012). Dendroecological studies
430 of climate-driven rates of tree growth are quickly shifting from assumptions of stationary tree-
431 climate relationships to demonstrations that climatic sensitivity varies across space and time
432 (Rollinson *et al.* in press; Thom *et al.* 2019; Peltier & Ogle 2020; Wilmking *et al.* 2020). By
433 focusing on spatial variations in ecosystem variability over the last millennium, our analyses
434 suggest spatial variation in ecosystem properties are a more important regulator than spatial

435 variations in climate exposure. Finally, uncertainties in the proxy-based reconstructions may
436 lower correlations as detrending techniques used to remove non-climatic signals such as age
437 effects may dampen estimates of centennial-scale variability (Allen *et al.* 2018; Esper *et al.*
438 2018). Despite lower PDSI variability in the LBDA than model drivers, we do not think that
439 spatial variability in hydroclimate variability in the empirical dataset is too low to detect effects on
440 ecosystem variability. Hydroclimate data syntheses for the last 2000 years and accompanying
441 EOF analyses suggest opposite loading patterns between MN/WI and New England, for both
442 principal components 2 & 3, which together explain 30% of variance in the hydroclimate records
443 (Shuman *et al.* 2019).

444 Process-based ecosystem models are the main vehicle for forecasting climate-driven
445 ecosystem dynamics across a range of timescales and in principle are better able to
446 accommodate past and future no-analog climates (Williams & Jackson 2007; Veloz *et al.* 2012).
447 However, all ecosystem models face tradeoffs in their ability to represent taxonomic or
448 functional diversity versus detailed ecophysiological processes that drive ecosystem change
449 (Fisher *et al.* 2018). Process-based ecosystems models will never be able to capture the full
450 complexity of ecosystems nor perfectly reproduce the patterns of climatological or ecological
451 variability observed in the past due to observational uncertainties and incomplete constraints of
452 many processes and parameterizations (Dietze 2017). This paper has shown how multiple
453 paleoecological data streams can be combined with harmonized paleoclimatic simulations and
454 multiple terrestrial ecosystem models to gain new insight into a) the patterns and controls on
455 past ecosystem variability and b) aspects of models such as diversity and demography where
456 complex representations are needed to achieve better agreement with the data. Nevertheless,
457 these analyses followed a traditional approach in which past ecosystem reconstructions and
458 simulations were run independently and compared at the final stage of analysis. The next major
459 step forward is to move to a full data-assimilation framework, in which paleoecological
460 observations and simulations are combined to provide joint estimates of state variables or better

461 constrain ecosystem model parameterizations (McLachlan & PalEON Project 2018). Through
462 this iterative process that draws upon an ever-growing and diversifying suite of observational
463 data streams (Farley *et al.* 2018), we can better understand the mechanisms regulating forest
464 sensitivity to climate variability across a broad range of timescales and thereby better forecast
465 future forest dynamics in a complex and rapidly changing world.

466

467 **Acknowledgements**

468 This work reflects the efforts of the Paleocological Observatory Network (PalEON Project),
469 funded by the National Science Foundation MacroSystems Biology under grants DEB-1241891,
470 DEB-1241868, DEB-1241874, and DEB-1241851 and special thanks to Jody Peters, PalEON
471 Project coordinator. PDSI calculations from ecosystem model drivers were derived from code
472 graciously provided by Ben Cook. Fossil pollen data were obtained from the Neotoma
473 Paleocology Database (<http://www.neotomadb.org>) and its constituent database the North
474 American Pollen Database. The work of the data contributors, data stewards, and the Neotoma
475 community is gratefully acknowledged.

476

477 **References**

- 478 Allen, C.D., Macalady, A.K., Chenchouni, H., Bachelet, D., McDowell, N., Vennetier, M., *et al.*
479 (2010). A global overview of drought and heat-induced tree mortality reveals emerging
480 climate change risks for forests. *For. Ecol. Manag.*, 259, 660–684.
- 481 Allen, K.J., Villalba, R., Lavergne, A., Palmer, J.G., Cook, E.C., Fenwick, P., *et al.* (2018). A
482 comparison of some simple methods used to detect unstable temperature responses in
483 tree-ring chronologies. *Dendrochronologia*, 48, 52–73.
- 484 Anav, A., Friedlingstein, P., Kidston, M., Bopp, L., Ciais, P., Cox, P., *et al.* (2013). Evaluating the
485 Land and Ocean Components of the Global Carbon Cycle in the CMIP5 Earth System
486 Models. *J. Clim.*, 26, 6801–6843.
- 487 Blarquez, O. & Aleman, J.C. (2016). Tree biomass reconstruction shows no lag in postglacial
488 afforestation of eastern Canada. *Can. J. For. Res.*, 46, 485–498.
- 489 Booth, R.K., Jackson, S.T., Sousa, V.A., Sullivan, M.E., Minckley, T.A. & Clifford, M.J. (2012).
490 Multi-decadal drought and amplified moisture variability drove rapid forest community
491 change in a humid region. *Ecology*, 93, 219–226.
- 492 Braconnot, P., Otto-Bliesner, B., Jungclaus, J. & Peterschmitt, J.-Y. (2011). The Paleoclimate
493 Modeling Intercomparison Project contribution to CMIP5. *CLIVAR Exch.*, 16, 15–19.

494 Breshears, D.D., Cobb, N.S., Rich, P.M., Price, K.P., Allen, C.D., Balice, R.G., *et al.* (2005).
495 Regional vegetation die-off in response to global-change-type drought. *Proc. Natl. Acad.*
496 *Sci.*, 102, 15144–15148.

497 Charney, N.D., Babst, F., Poulter, B., Record, S., Trouet, V.M., Frank, D., *et al.* (2016).
498 Observed forest sensitivity to climate implies large changes in 21st century North
499 American forest growth. *Ecol. Lett.*, 19, 1119–1128.

500 Clifford, M.J. & Booth, R.K. (2015). Late-Holocene drought and fire drove a widespread change
501 in forest community composition in eastern North America. *The Holocene*, 25, 1102–
502 1110.

503 Cook, B.I., Ault, T.R. & Smerdon, J.E. (2015). Unprecedented 21st century drought risk in the
504 American Southwest and Central Plains. *Sci. Adv.*, 1, e1400082.

505 Cook, E.R., Seager, R., Heim, R.R., Vose, R.S., Herweijer, C. & Woodhouse, C. (2010).
506 Megadroughts in North America: placing IPCC projections of hydroclimatic change in a
507 long-term palaeoclimate context. *J. Quat. Sci.*, 25, 48–61.

508 Dawson, A., Goring, S., Paciorek, C.J., Jackson, S.T., McLachlan, J.S. & Williams, J.W.
509 (2019a). *STEPPS 2000 Year Forest Composition Estimates, Upper Midwest US, Level*
510 *2*. Environmental Data Initiative.

511 Dawson, A., Paciorek, C.J., Goring, S.J., Jackson, S.T., McLachlan, J.S. & Williams, J.W.
512 (2019b). Quantifying trends and uncertainty in prehistoric forest composition in the upper
513 Midwestern United States. *Ecology*, 100.

514 Dawson, A., Paciorek, C.J., McLachlan, J.S., Goring, S., Williams, J.W. & Jackson, S.T. (2016).
515 Quantifying pollen-vegetation relationships to reconstruct ancient forests using 19th-
516 century forest composition and pollen data. *Quat. Sci. Rev.*, 137, 156–175.

517 Dawson, T.P., Jackson, S.T., House, J.I., Prentice, I.C. & Mace, G.M. (2011). Beyond
518 predictions: biodiversity conservation in a changing climate. *Science*, 332.

519 De Kauwe, M.G., Medlyn, B.E., Zaehle, S., Walker, A.P., Dietze, M.C., Hickler, T., *et al.* (2013).
520 Forest water use and water use efficiency at elevated CO₂: a model-data
521 intercomparison at two contrasting temperate forest FACE sites. *Glob. Change Biol.*, 19,
522 1759–1779.

523 Dietze, M.C. (2017). Prediction in ecology: a first-principles framework. *Ecol. Appl.*, 27, 2048–
524 2060.

525 Dietze, M.C., Fox, A., Beck-Johnson, L.M., Betancourt, J.L., Hooten, M.B., Jarnevich, C.S., *et*
526 *al.* (2018). Iterative near-term ecological forecasting: Needs, opportunities, and
527 challenges. *Proc. Natl. Acad. Sci.*, 115, 1424–1432.

528 Esper, J., George, S.St., Anchukaitis, K., D'Arrigo, R., Ljungqvist, F.C., Luterbacher, J., *et al.*
529 (2018). Large-scale, millennial-length temperature reconstructions from tree-rings.
530 *Dendrochronologia*, 50, 81–90.

531 Evans, M.N., Tolwinski-Ward, S.E., Thompson, D.M. & Anchukaitis, K.J. (2013). Applications of
532 proxy system modeling in high resolution paleoclimatology. *Quat. Sci. Rev.*, 76, 16–28.

533 Farley, S.S., Dawson, A., Goring, S.J. & Williams, J.W. (2018). Situating Ecology as a Big-Data
534 Science: Current Advances, Challenges, and Solutions. *BioScience*, 68, 563–576.

535 Fisher, R.A., Koven, C.D., Anderegg, W.R.L., Christoffersen, B.O., Dietze, M.C., Farnior, C.E., *et*
536 *al.* (2018). Vegetation demographics in Earth System Models: A review of progress and
537 priorities. *Glob. Change Biol.*, 24, 35–54.

538 Friedlingstein, P., Cox, P., Betts, R., Bopp, L., von Bloh, W., Brovkin, V., *et al.* (2006). Climate–
539 Carbon Cycle Feedback Analysis: Results from the C⁴ MIP Model Intercomparison. *J.*
540 *Clim.*, 19, 3337–3353.

541 Friedlingstein, P., Meinshausen, M., Arora, V.K., Jones, C.D., Anav, A., Liddicoat, S.K., *et al.*
542 (2014). Uncertainties in CMIP5 Climate Projections due to Carbon Cycle Feedbacks. *J.*
543 *Clim.*, 27, 511–526.

544 Goring, S.J., Mladenoff, D.J., Cogbill, C.V., Record, S., Paciorek, C.J., Jackson, S.T., *et al.*
545 (2016). Novel and Lost Forests in the Upper Midwestern United States, from New
546 Estimates of Settlement-Era Composition, Stem Density, and Biomass. *PLOS ONE*, 11,
547 e0151935.

548 Keeley, J.E., van Mantgem, P. & Falk, D.A. (2019). Fire, climate and changing forests. *Nat.*
549 *Plants*, 5, 774–775.

550 Klesse, S., Babst, F., Lienert, S., Spahni, R., Joos, F., Bouriaud, O., *et al.* (2018). A Combined
551 Tree Ring and Vegetation Model Assessment of European Forest Growth Sensitivity to
552 Interannual Climate Variability. *Glob. Biogeochem. Cycles*.

553 Kujawa, E.R., Goring, S., Dawson, A., Calcote, R., Grimm, E.C., Hotchkiss, S.C., *et al.* (2016).
554 The effects of anthropogenic land cover change on pollen-vegetation relationships in the
555 American Midwest. *Anthropocene*, 15, 60–71.

556 Kumar, J., Brooks, B.-G.J., Thornton, P.E. & Dietze, M.C. (2012). Sub-daily Statistical
557 Downscaling of Meteorological Variables Using Neural Networks. *Procedia Comput.*
558 *Sci.*, 9, 887–896.

559 LeBauer, D.S., Wang, D., Richter, K.T., Davidson, C.C. & Dietze, M.C. (2013). Facilitating
560 feedbacks between field measurements and ecosystem models. *Ecol. Monogr.*, 83,
561 133–154.

562 Liu, F., Mladenoff, D.J., Keuler, N.S. & Moore, L.S. (2011). BROADSCALE variability in tree data of
563 the historical Public Land Survey and its consequences for ecological studies. *Ecol.*
564 *Monogr.*, 81, 259–275.

565 Matthes, J.H., Goring, S., Williams, J.W. & Dietze, M.C. (2016). Benchmarking historical CMIP5
566 plant functional types across the Upper Midwest and Northeastern United States. *J.*
567 *Geophys. Res. Biogeosciences*, 121, 523–535.

568 McCabe, T.D. & Dietze, M.C. (2019). Scaling Contagious Disturbance: A Spatially-Implicit
569 Dynamic Model. *Front. Ecol. Evol.*, 7.

570 McLachlan, J.S. & PalEON Project. (2018). Forecasting long-term ecological dynamics using
571 open paleodata. *Past Glob. Change Mag.*, 26, 76–76.

572 Medlyn, B.E., Zaehle, S., De Kauwe, M.G., Walker, A.P., Dietze, M.C., Hanson, P.J., *et al.*
573 (2015). Using ecosystem experiments to improve vegetation models. *Nat. Clim. Change*,
574 5, 528–534.

575 Nolan, C., Overpeck, J.T., Allen, J.R.M., Anderson, P.M., Betancourt, J.L., Binney, H.A., *et al.*
576 (2018). Past and future global transformation of terrestrial ecosystems under climate
577 change. *Science*, 361, 920–923.

578 Paciorek, C.J., Cogbill, C.V., Peters, J.A., Goring, S.J., Williams, J.W., Mladenoff, D.J., *et al.*
579 (2019). *Statistically-estimated tree biomass, stem density, and basal area for the upper*
580 *Midwestern United States at the time of Euro-American settlement* (preprint). *Ecology*.

581 Paciorek, C.J., Goring, S.J., Thurman, A.L., Cogbill, C.V., Williams, J.W., Mladenoff, D.J., *et al.*
582 (2016). Statistically-Estimated Tree Composition for the Northeastern United States at
583 Euro-American Settlement. *PLOS ONE*, 11, e0150087.

584 Paciorek, C.J. & McLachlan, J.S. (2009). Mapping Ancient Forests: Bayesian Inference for
585 Spatio-Temporal Trends in Forest Composition Using the Fossil Pollen Proxy Record. *J.*
586 *Am. Stat. Assoc.*, 104, 608–622.

587 Peltier, D.M.P. & Ogle, K. (2020). Tree growth sensitivity to climate is temporally variable. *Ecol.*
588 *Lett.*, 1–20.

589 Pelton, W.L., King, K.M. & Tanner, C.B. (1960). An evaluation of the Thornthwaite and mean
590 temperature methods for determining potential evapotranspiration. *Agron. J.*, 52, 387–
591 395.

592 Raiho, A.M., Paciorek, C.J. & McLachlan, J.S. (in prep). Species migrations created a 5,000
593 year regional carbon sink past.

594 Rollinson, C.R., Finley, A.O., Alexander, M.R., Banerjee, S., Dixon Hamil, K.-A., Koenig, L., *et*
595 *al.* (in press). Working across space and time: nonstationarity in ecological research and
596 application. *Front. Ecol. Environ.*

597 Rollinson, C.R., Liu, Y., Raiho, A., Moore, D.J.P., McLachlan, J., Bishop, D.A., *et al.* (2017).
598 Emergent climate and CO₂ sensitivities of net primary productivity in ecosystem models
599 do not agree with empirical data in temperate forests of eastern North America. *Glob.*
600 *Change Biol.*, 23, 2755–2767.

601 Schimel, D., Stephens, B.B. & Fisher, J.B. (2015). Effect of increasing CO₂ on the terrestrial
602 carbon cycle. *Proc. Natl. Acad. Sci.*, 112, 436–441.

603 Seidl, R., Fernandes, P.M., Fonseca, T.F., Gillet, F., Jönsson, A.M., Merganičová, K., *et al.*
604 (2011). Modelling natural disturbances in forest ecosystems: a review. *Ecol. Model.*, 222,
605 903–924.

606 Shuman, B., Newby, P., Huang, Y. & Webb, T. (2004). Evidence for the close climatic control of
607 New England vegetation history. *Ecology*, 85, 1297–1310.

608 Shuman, B.N., Marsicek, J., Oswald, W.W. & Foster, D.R. (2019). Predictable hydrological and
609 ecological responses to Holocene North Atlantic variability. *Proc. Natl. Acad. Sci.*, 116,
610 5985–5990.

611 Simpson, G.L. (2018). Modelling Palaeoecological Time Series Using Generalised Additive
612 Models. *Front. Ecol. Evol.*, 6.

613 Taylor, K.E., Stouffer, R.J. & Meehl, G.A. (2012). An Overview of CMIP5 and the Experiment
614 Design. *Bull. Am. Meteorol. Soc.*, 93, 485–498.

615 Thom, D., Golivets, M., Edling, L., Meigs, G.W., Gourevitch, J.D., Sonter, L.J., *et al.* (2019). The
616 climate sensitivity of carbon, timber, and species richness covaries with forest age in
617 boreal–temperate North America. *Glob. Change Biol.*, 25, 1446–2458.

618 Thornthwaite, C.W. & Mather, J.R. (1957). Instructions and tables for computing potential
619 evapotranspiration and the water balance. *Publ. Climatol.*, 10, 185–311.

620 Trachsel, M., Dawson, A., Paciorek, C.J., Williams, J.W., McLachlan, J.S., Cogbill, C.V., *et al.*
621 (2020). Comparison of settlement-era vegetation reconstructions for STEPPS and
622 REVEALS pollen–vegetation models in the northeastern United States. *Quat. Res.*, 95,
623 23–42.

624 Veloz, S.D., Williams, J.W., Blois, J.L., He, F., Otto-Bliesner, B. & Liu, Z. (2012). No-analog
625 climates and shifting realized niches during the late quaternary: implications for 21st-
626 century predictions by species distribution models. *Glob. Change Biol.*, 18, 1698–1713.

627 Walker, A.P., Hanson, P.J., De Kauwe, M.G., Medlyn, B.E., Zaehle, S., Asao, S., *et al.* (2014).
628 Comprehensive ecosystem model-data synthesis using multiple data sets at two
629 temperate forest free-air CO₂ enrichment experiments: Model performance at ambient
630 CO₂ concentration: FACE MODEL-DATA SYNTHESIS. *J. Geophys. Res.*
631 *Biogeosciences*, 119, 937–964.

632 Walker, A.P., Zaehle, S., Medlyn, B.E., De Kauwe, M.G., Asao, S., Hickler, T., *et al.* (2015).
633 Predicting long-term carbon sequestration in response to CO₂ enrichment: How and
634 why do current ecosystem models differ? *Glob. Biogeochem. Cycles*, 29, 476–495.

635 Wei, Y., Liu, S., Huntzinger, D.N., Michalak, A.M., Viogy, N., Post, W.M., *et al.* (2014). The
636 North American Carbon Program Multi-scale Synthesis and Terrestrial Model
637 Intercomparison Project – Part 2: Environmental driver data. *Geosci. Model Dev.*, 7,
638 2875–2893.

639 Williams, J.W., Blois, J.L. & Shuman, B.N. (2011). Extrinsic and intrinsic forcing of abrupt
640 ecological change: case studies from the late Quaternary: Extrinsic and intrinsic abrupt
641 ecological change. *J. Ecol.*, 99, 664–677.

642 Williams, J.W. & Jackson, S.T. (2007). Novel Climates, No-Analog Communities, and Ecological
643 Surprises. *Front. Ecol. Environ.*, 5, 475–482.

644 Wilmking, M., Maaten-Theunissen, M., Maaten, E., Scharnweber, T., Buras, A., Biermann, C., *et*
645 *al.* (2020). Global assessment of relationships between climate and tree growth. *Glob.*
646 *Change Biol.*, 26, 3212–3220.

647 Wood, S.N. (2017). *Generalized Additive Models: An Introduction with R*. 2nd edn. Chapman
648 and Hall/CRC, New York.

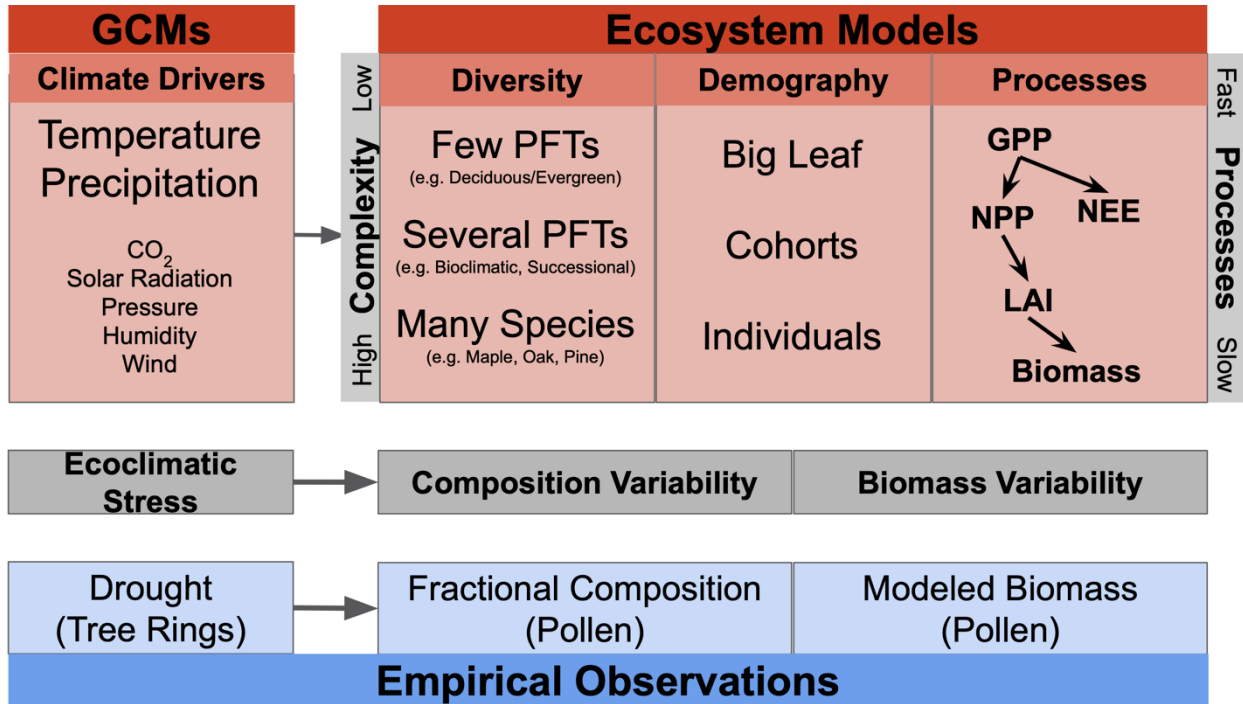
649 Woodhouse, C.A., Meko, D.M., MacDonald, G.M., Stahle, D.W. & Cook, E.R. (2010). A 1,200-
650 year perspective of 21st century drought in southwestern North America. *Proc. Natl.*
651 *Acad. Sci.*, 107, 21283–21288.

652

653 **Manuscript Tables**

654 **Table 1:** Comparison of 1) ecosystem model complexity, based on representation of diversity,
 655 demographic, and ecophysiological processes with 2) variability in forest composition and
 656 biomass and sensitivity to hydroclimate variability. Compositional and biomass variability (Log
 657 Comp. Var.; Log Biom. Var) are represented by log-transformed mean and standard deviation
 658 across space of temporal variability, represented in turn as the sum of centennially-resolved first
 659 differences of fractional composition of the dominant plant type or aboveground biomass.
 660 Composition and biomass sensitivity are represented as the mean slope and standard error of
 661 log-log regression between composition or biomass variability and hydroclimate variability. PFT
 662 = plant functional types. For sensitivity columns, * indicates slopes significantly different from
 663 zero ($p < 0.05$); † indicates model slope significantly different from pollen ($p < 0.05$).

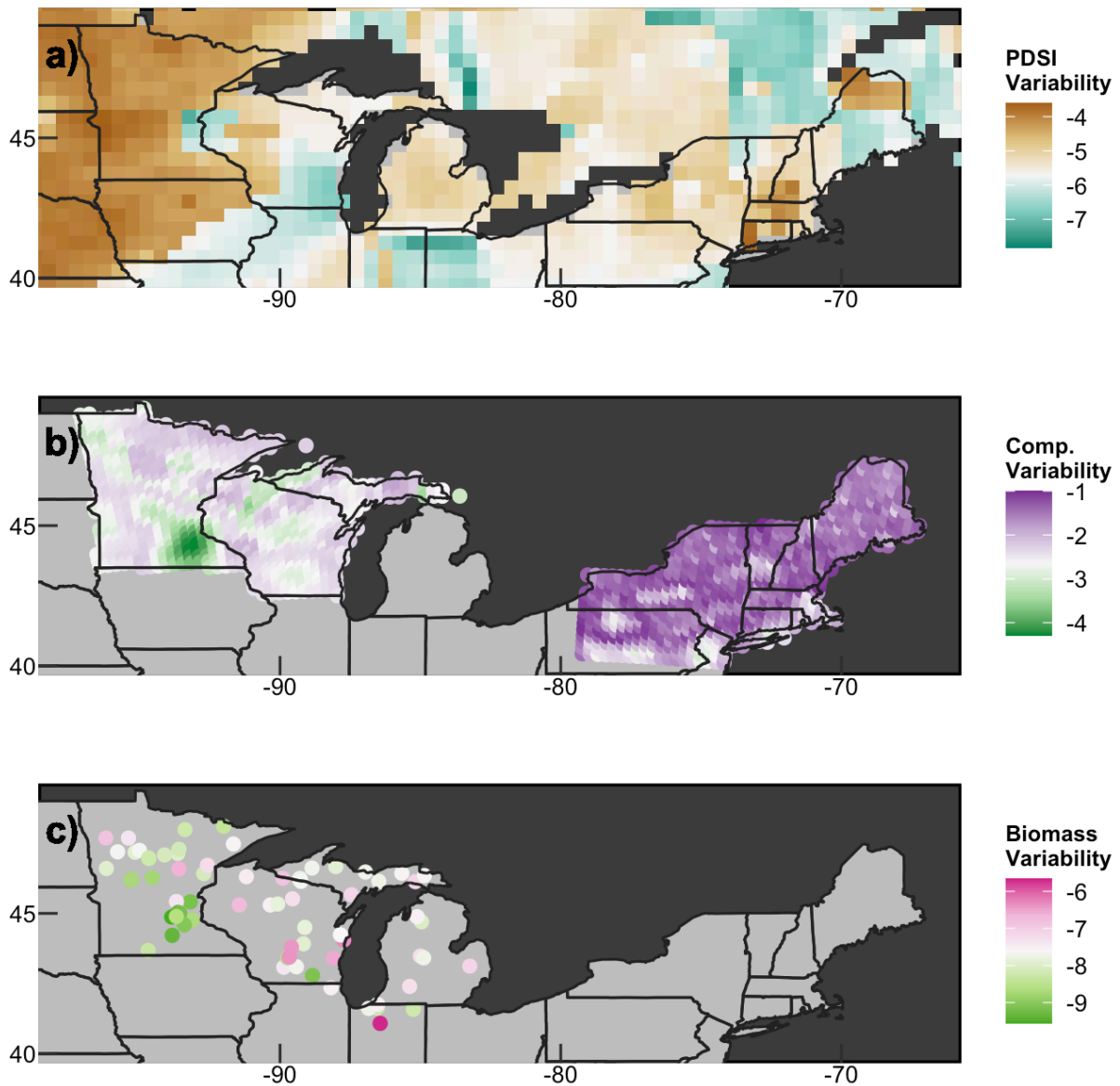
Data Source & Model Name	Tree Diversity Representation	Demographic Representation	Vegetation Processes	Comp. Var. (log)	Comp. Sens. (log-log)	Biom. Var. (log)	Biom. Sens. (log-log)
Pollen: STEPPS, ReFAB	Genera: 12 trees	relative abundance	[implicit]	-2.032 (0.617)	0.026 (0.019)	-7.798 (0.770)	-0.156 (0.119)
ED2	PFTs: 5 tree	cohort	photosynthesis, allocation, cross-PFT competition, cross-cohort competition	-7.156 (0.514)	0.118 (0.018)*†	-7.505 (0.446)	-0.079 (0.027)*
LINK-AGES	Species: 15 tree	individual	cross-PFT competition, cross-cohort competition	-6.598 (0.478)	0.074 (0.018)*	-6.741 (0.999)	0.230 (0.028)*†
LPJ-GUESS	PFTs: 6 tree, 1 grass	cohort	photosynthesis, allocation, cross-PFT competition, cross-cohort competition	-7.290 (0.452)	0.056 (0.018)*	-7.379 (0.597)	-0.069 (0.027)*
LPJ-WSL	PFTs: 5 tree, 1 grass	cohort	photosynthesis, allocation, cross-PFT competition, cross-cohort competition	-7.829 (0.943)	0.252 (0.018)*†	-7.106 (0.964)	-0.020 (0.027)
JULES-TRIFFID	PFTs: 2 Tree, 2 grass, 1 shrub	PFT	Photosynthesis, allocation, cross-PFT competition	-8.633 (1.075)	0.411 (0.022)*†	-8.639 (0.952)	0.203 (0.033)*†



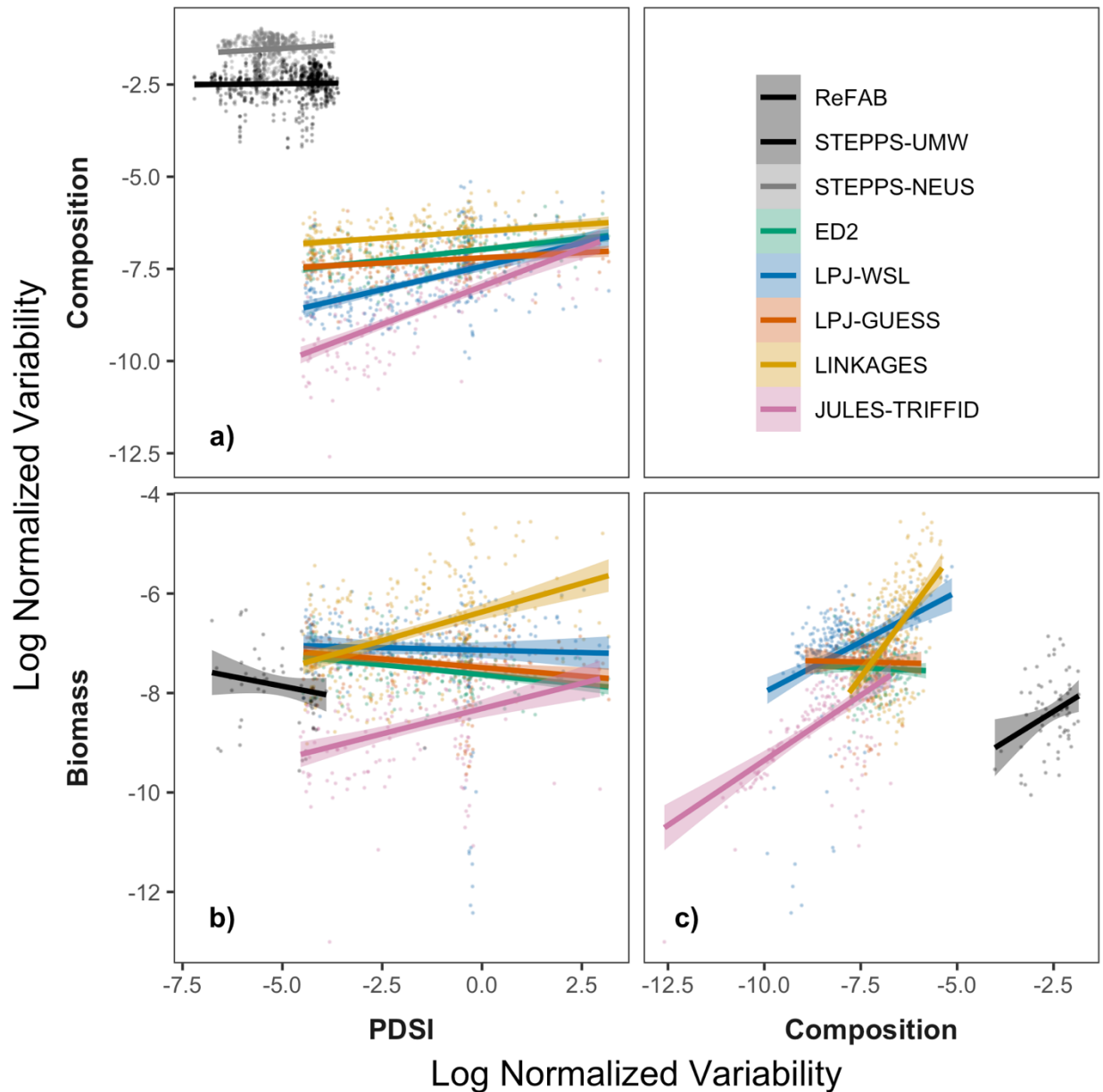
666
 667 **Figure 1:** Overview of the unified conceptual framework (gray boxes) for parallel analysis of
 668 empirical data (blue boxes) and model output (red boxes). For ecosystem models, we describe
 669 the latent climatic and ecosystem processes that are unobservable in paleoecological data and
 670 differences among models in complexity. Complexity here is organized into three categories: 1)
 671 diversity, ranging from a few plant functional types (PFTs) to many species; 2) demography,
 672 ranging from ‘big leaf’ models with no explicit treatment of forest demography to models with
 673 individual trees; and 3) ecophysiological processes. Changes in forest biomass emerge from
 674 latent ecophysiological processes including gross primary productivity (GPP), net primary
 675 productivity (NPP), net ecosystem exchange (NEE), and leaf area index (LAI). Ecophysiological
 676 processes are controlled by model representation of higher-level vegetation processes (Table
 677 1). Latent model drivers, processes, and states (red boxes) result in estimates of forest
 678 composition and biomass that can be compared to paleoecological data products (blue boxes).
 679 Models vary in complexity due to design philosophy and tradeoffs between model complexity
 680 and computational speed.

681

682



683
 684 **Figure 2:** Spatial distribution of inferred temporal variability for 850 to 1850 AD for a) drought
 685 (PDSI) from the Living Blended Drought Atlas (44), b) forest composition from the STEPPS
 686 pollen-vegetation model (8, 24), and c) forest aboveground biomass from the ReFab pollen-
 687 biomass model (7). All variability estimates were divided by mean to facilitate inter-variable
 688 comparison (*Methods*). Spatial extent of compositional and biomass reconstructions are
 689 uneven across the study domain, as is the temporal extent of reconstructed drought variability
 690 (Supplemental Figure 1). Empirical comparisons of composition or biomass variability with
 691 drought variability are restricted to the common temporal extents for each location.
 692



695

696

697 **Figure 3:** Inferred (black, gray) and simulated (colors) sensitivity of variability of forest

698 composition and biomass to ecohydrological variability (PDSI) (a,b) and of biomass variability to

699 compositional variability (c). Inferred variables suggest weak to no correlation (low sensitivity)

700 between climate variability and ecosystem variability (composition and biomass). In contrast,

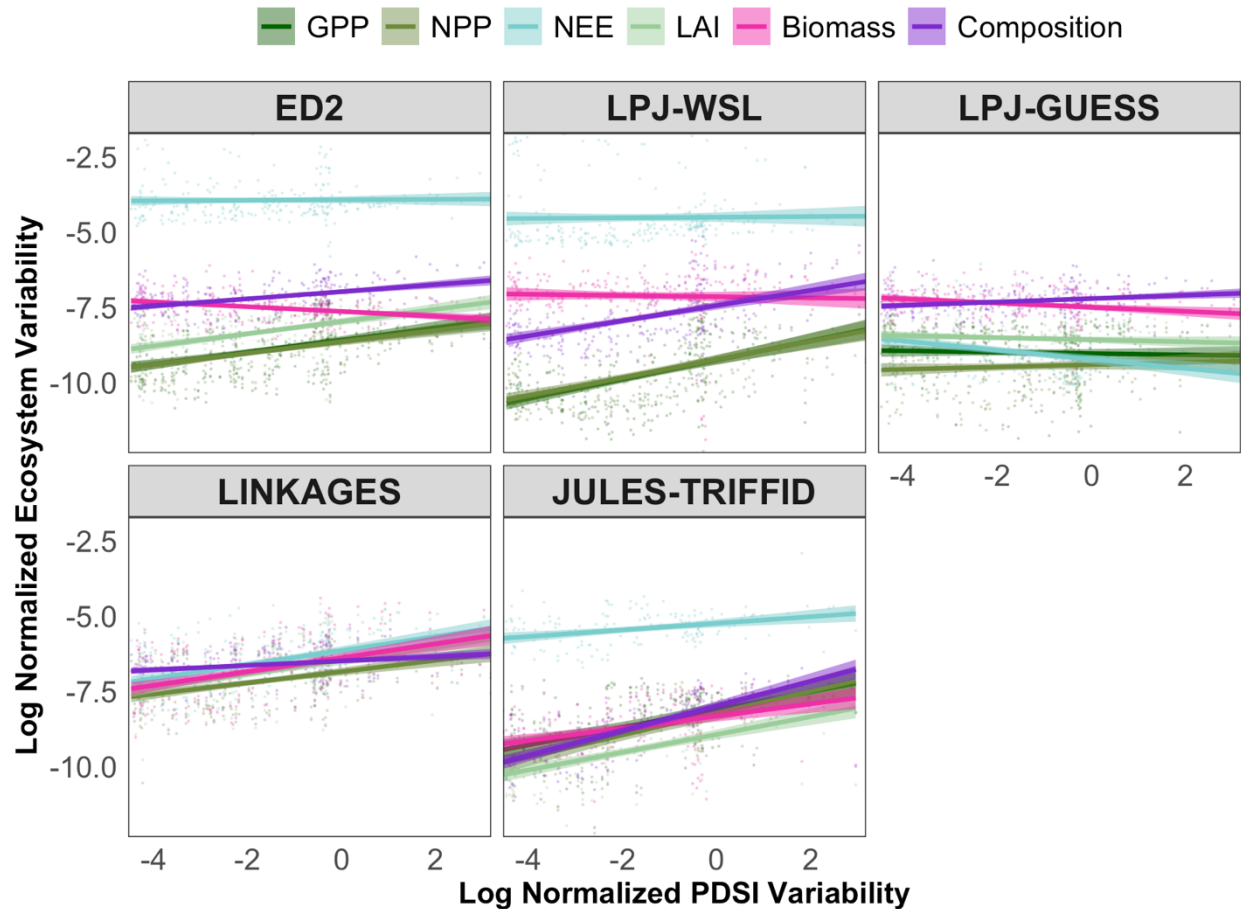
701 ecosystem models generally simulate higher sensitivity of ecosystems to climate variability.

702 Inferred compositional (STEPPS) and biomass (ReFAB) variabilities are positively correlated,

703 while this relationship varied among models.

704

704



705
706
707
708
709
710
711
712
713

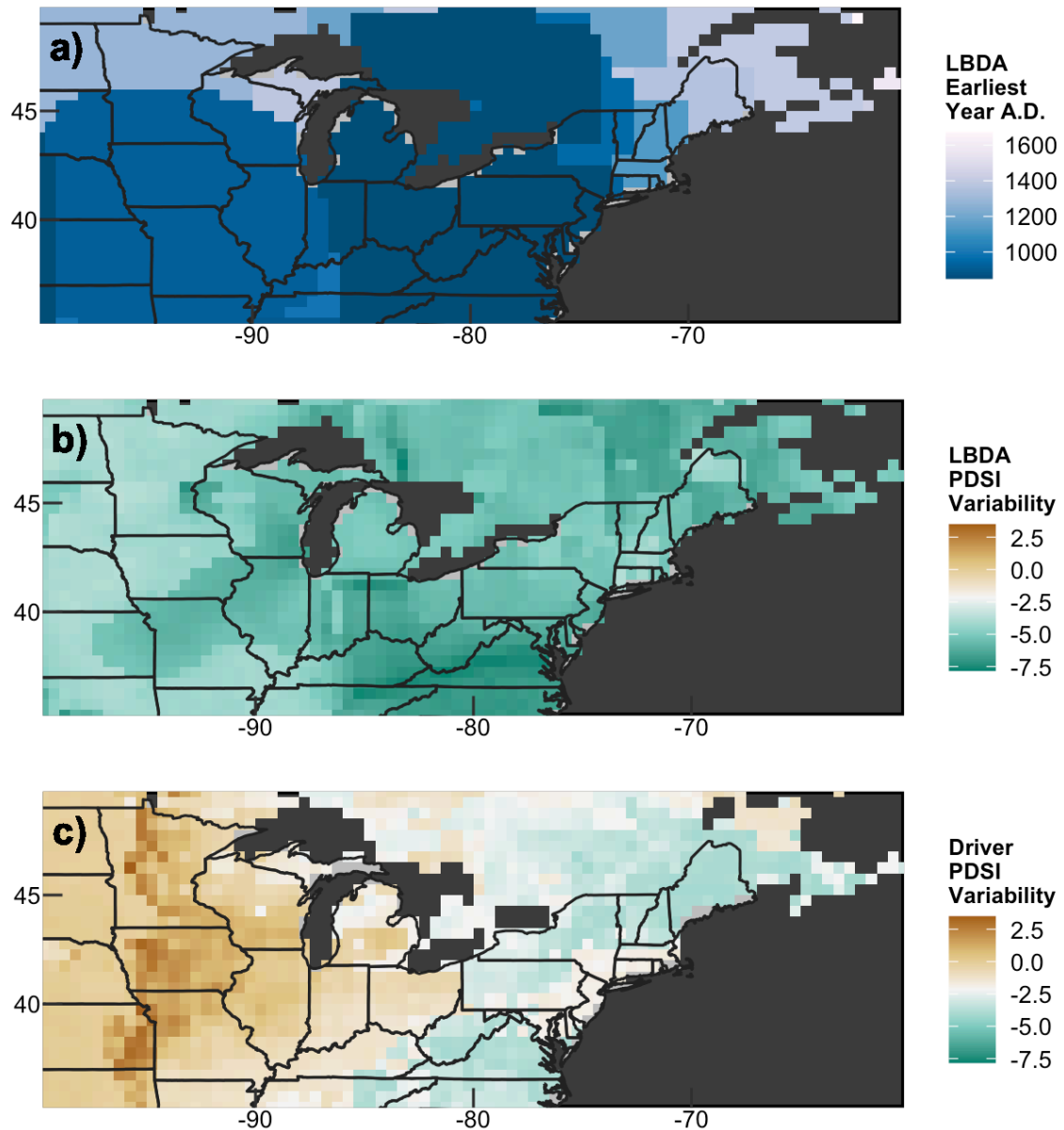
Figure 4: Diagnosing the observed and latent relationships among ecohydrological variability and variability in forest composition, structure, and function in five terrestrial ecosystem models (ED2, LPJ-WSL, LPJ-GUESS, LINKAGES, and JULES-TRIFFID). All models showed positive correlations between composition and drought variability, but some models showed positive biomass sensitivities (LINKAGES, JULES-TRIFFID) while others were negative (ED2, LPJ-WSL, LPJ-GUESS). In all models, composition sensitivity to hydroclimate variability was most similar to NPP whereas biomass sensitivity tended to mirror NEE.

714 **Supplemental Tables**

715 **Supplemental Table 1:** Sensitivity of latent state variability to hydroclimate (PDSI) variability in
 716 ecosystem models and pollen data products. Sensitivity is presented as the mean and standard
 717 error slope from log-log regression; * indicates slopes significantly different from zero (p<0.05).
 718 LINKAGES does not simulate GPP. LAI output was not available for LPJ-WSL.

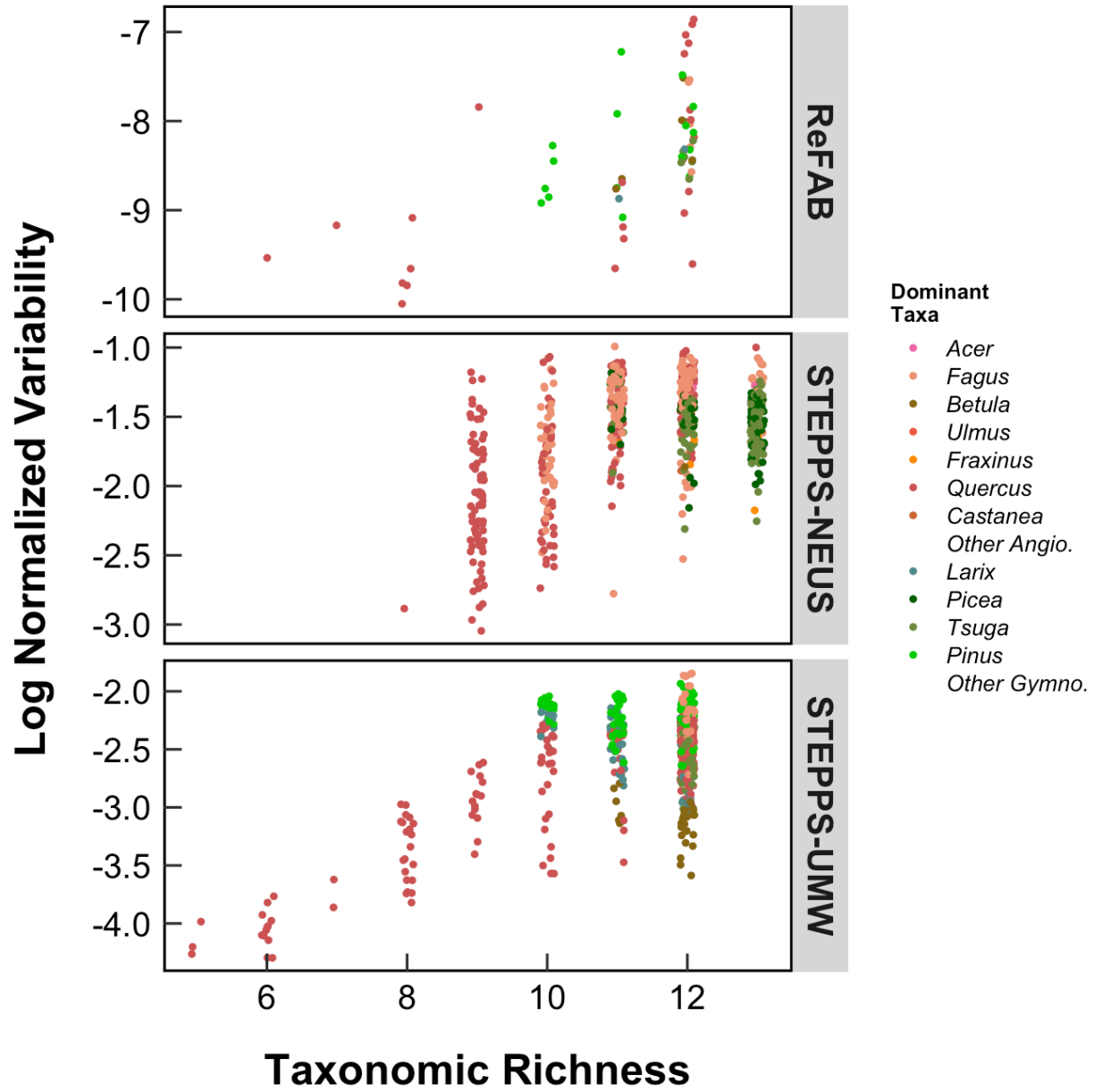
Model	GPP	NPP	NEE	LAI	Biomass	Composition
Pollen					-0.156 (0.119)	0.026 (0.019)
ED2	0.201 (0.028)*	0.190 (0.025)*	0.008 (0.024)	0.203 (0.024)*	-0.079 (0.015)*	0.118 (0.017)*
LPJ-WSL	0.320 (0.033)*	0.301 (0.033)*	0.010 (0.034)		-0.020 (0.034)	0.252 (0.029)*
LPJ-GUESS	-0.022 (0.031)	0.038 (0.034)	-0.152 (0.031)*	-0.034 (0.022)	-0.069 (0.020)*	0.056 (0.015)*
LINKAGES		0.186 (0.027)*	0.232 (0.030)*	0.222 (0.031)*	0.230 (0.033)*	0.074 (0.016)*
JULES-TRIFFID	0.294 (0.051)*	0.365 (0.051)*	0.110 (0.028)*	0.295 (0.035)*	0.203 (0.038)*	0.411 (0.033)*

720 **Supplemental Figures**



721 **Supplemental Figure 1:** Comparison of log normalized PDSI variability in empirically-inferred
722 reconstructions from the Living Blended Drought Atlas (LBDA, 41, a, b) and model drivers (c).
723 Due to the regional differences in the length of tree-ring chronologies available for PDSI
724 reconstruction, the temporal extent of analyses involving LBDA drought is uneven across space.
725 Overall, model drivers had greater PDSI variability than seen in the LBDA, but both datasets
726 show greater variability in the western region of the study domain.
727
728

729



730
731
732
733

Supplemental Figure 2: Relationship between taxonomic richness and log normalized biomass (ReFAB) and composition (STEPPS) variability in pollen-inferred datasets.